6.2.1 Corrections for the Four-Jet Observables

Background plus Hadronization Corrections

The theoretical NLO prediction as obtained from DEBRECEN should be corrected for background and hadronization effects. The correction procedure was detailed in Section 5.3.1. In Fig. 6.9 the background plus hadronization corrections as obtained from PYTHIA and HERWIG are shown.

The background plus hadronization corrections from the HERWIG simulation show large discrepancies with respect to the ones coming from PYTHIA. The showering and hadronization parameters used, both in HERWIG and PYTHIA, are the standard ones, which were obtained by the tuning of MC simulations starting from $q\bar{q}$ configurations. Therefore this may be an indication of the non-universality of these parameters. If a better tuning cannot be found, then the reason for the discrepancies could be due to the implementation of the showering and hadronization processes in the MC programs. More detailed studies about the four-parton Monte Carlo programs are presented in Chapter 7.

Detector Corrections

The theoretical prediction for the four-jet angular correlations, already corrected for hadronization effects, has to be corrected further to include detector effects before being compared to ALEPH data. This is done by computing these observables from the MC before and after simulation, and the corrections are found in Fig. 6.10. In the case of $\cos\alpha_{34}$ the detector corrections calculated from the simulation with the PYTHIA four-parton option passed through the detector simulation is also shown. This, as explained in Section 5.3.2, is the one used for the systematic uncertainty estimation.

Total Corrections

Taking into account the hadronization and detector corrections as explained in the previous chapter, the total corrections for each four-jet observable can be constructed as

$$C^{\mathrm{tot}}(i_{bin}) = C^{\mathrm{bck+had}}(i_{bin}) \cdot C^{\mathrm{det}}(i_{bin}) \,. \tag{6.2}$$

Figure 6.11 shows the total bin-by-bin corrections for the angular correlations when using PYTHIA for the hadronization corrections. Typically such corrections are found within the 5-10% range. The corrections for the four-jet rate can be found in Fig. 6.3.

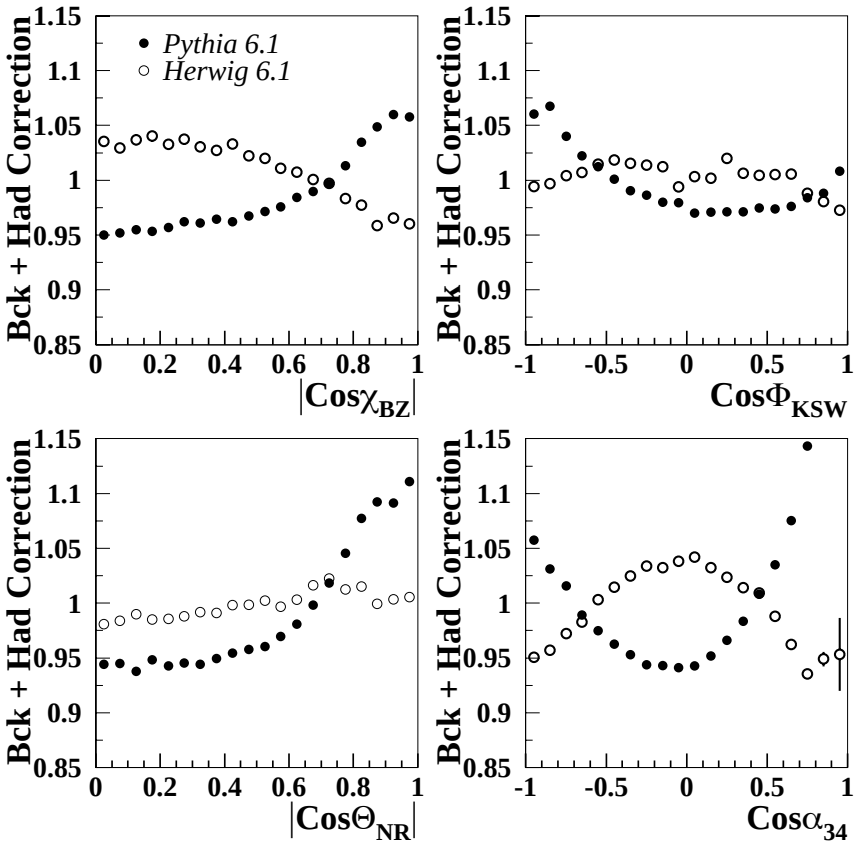

Figure 6.9: Background and hadronization corrections for the four-jet angular correlations.

6.2.2 Results

An experimental covariance matrix is calculated to take into account the statistical error of the data, the statistical errors of the detector and hadronization corrections, and the bin-by-bin statistical correlations among the different observables as well as the correlations between the bins of a single observable. Tables 6.13-6.16 show the data distributions for the four-jet angular correlations from ALEPH. Results for the four-jet rate can be found in Table 6.1. The correlations among the angular abservables are displayed in Fig. 6.12, where the correlations reach values higher than 50% for some bins.

Then a χ^2 minimization is performed with respect to η, x and y, using statistical errors only. The fit range is selected by requiring the total corrections for each observable

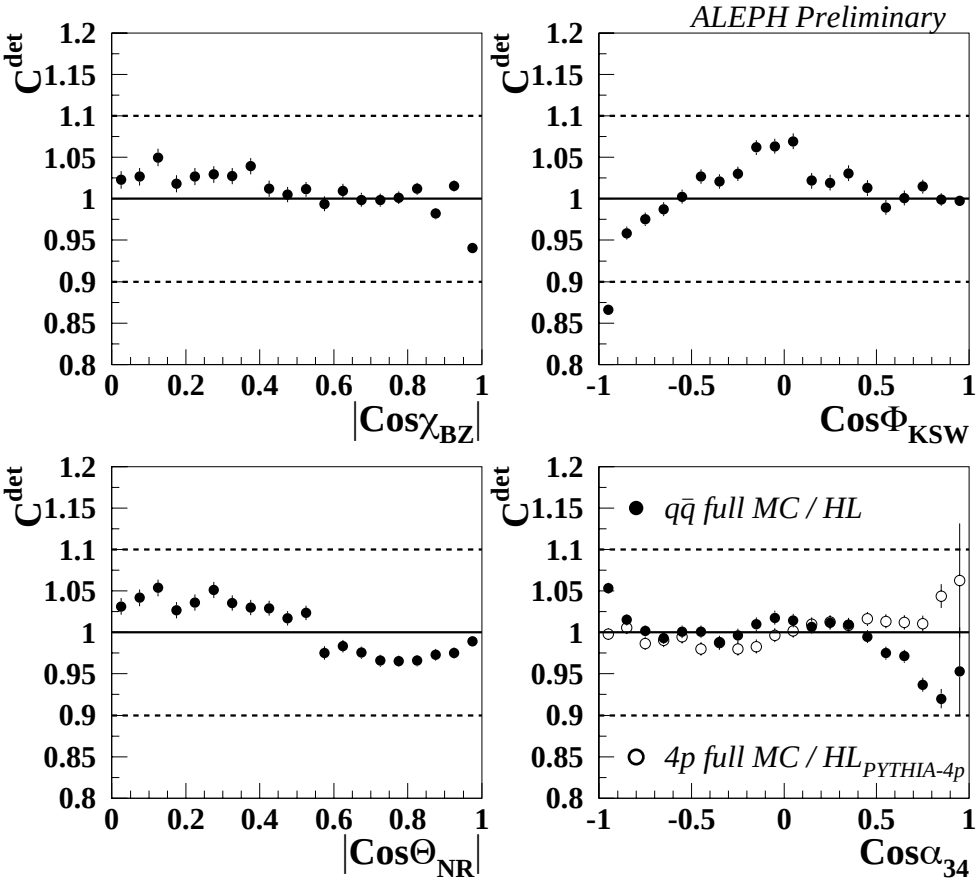

Figure 6.10: Detector corrections for the four-jet angular correlations.

to be smaller than 10%.

The results are seen in Table 6.17, and show good agreement with both QCD expectations and previous results [21] [55]. However, an important reduction of the statistical error is achieved. In the previous ALEPH analysis, the normalization of the four-jet angular correlations was also fitted, which prevented from achieving a better statistical precision. The fact that different observables were used should also be taken into account when comparing to the results in this thesis. The comparison with the OPAL results should be done after considering the smaller amount of MC used in that case for the hadronization and detector corrections, as well as the differences in the fit ranges for the angular correlations.

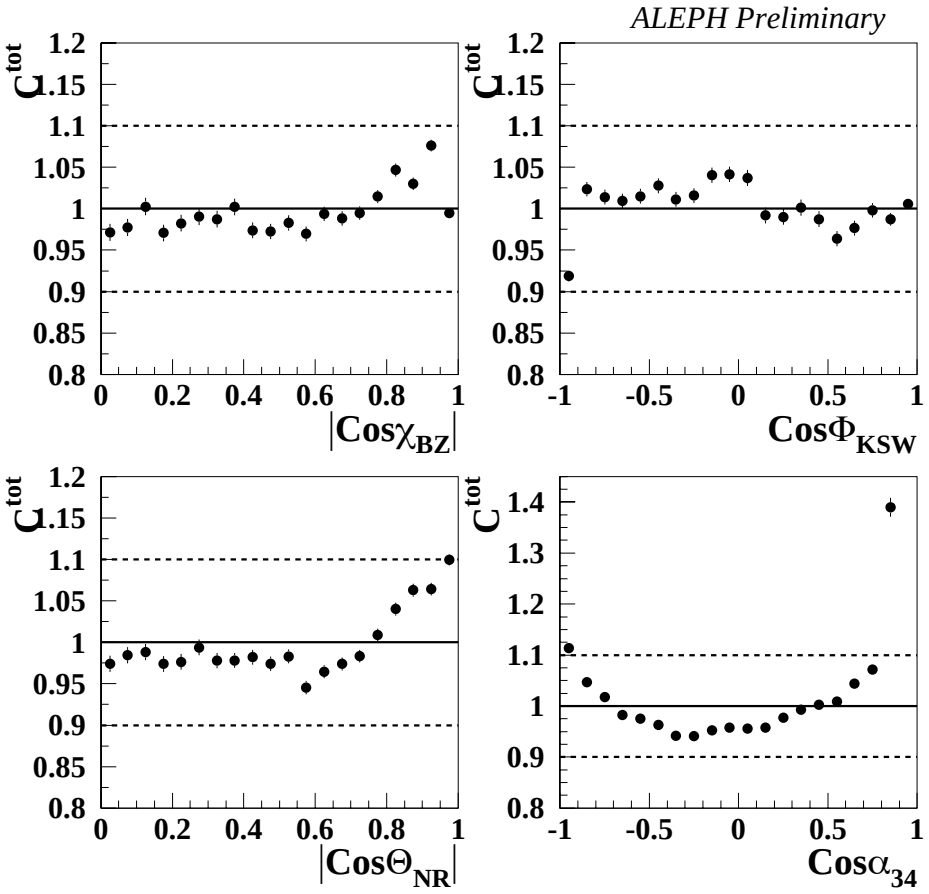

Figure 6.11: Total corrections for the four-jet angular correlations. The dashed lines show the maximum allowed corrections used for the fit.

The fitted distributions can be seen in Figs. 6.13 and 6.14. In the case of $\cos\alpha_{34}$ a significant discrepancy in the central region of the distributions is observed. This disagreement was already seen in [55]. Its origin is not understood. For the four-jet rate, the disagreement between the fitted predictions at small values of y_{cut} are again observed.

6.2.3 Systematic Studies

Tables 6.18-6.22 show the systematic uncertainties that have been studied. A brief description of each of them can be found in the following paragraphs.

Center of bin	N_{events} (ALEPH data)	N_{events} (full MC)	N_{events} (at HL)
0.025	5812 ± 74.86	10427 ± 100.45	79225 ± 277.04
0.075	5639 ± 73.78	10492 ± 100.77	79417 ± 277.37
0.125	5554 ± 73.24	10898 ± 102.64	80675 ± 279.48
0.175	5665 ± 73.95	10771 ± 102.06	82210 ± 282.04
0.225	5795 ± 74.76	11118 ± 103.63	84147 ± 285.23
0.275	5872 ± 75.24	11341 ± 104.63	85610 ± 287.61
0.325	5938 ± 75.64	11679 ± 106.12	88343 ± 292.01
0.375	5926 ± 75.57	12235 ± 108.52	91475 ± 296.95
0.425	6079 ± 76.50	12280 ± 108.71	94282 ± 301.30
0.475	6197 ± 77.21	12655 ± 110.29	97842 ± 306.71
0.525	6607 ± 79.62	13406 ± 113.38	103005 ± 314.36
0.575	6991 ± 81.80	13846 ± 115.15	108251 ± 321.92
0.625	7297 ± 83.49	14715 ± 118.54	113282 ± 328.98
0.675	7742 ± 85.87	15617 ± 121.94	121505 ± 340.13
0.725	8122 ± 87.85	16768 ± 126.12	130519 ± 351.86
0.775	8929 ± 91.87	18295 ± 131.41	141982 ± 366.11
0.825	9862 ± 96.26	20311 ± 138.01	155978 ± 382.61
0.875	10967 ± 101.14	22195 ± 143.83	175600 ± 404.29
0.925	12831 ± 108.72	26429 ± 155.85	202268 ± 431.45
0.975	25138 ± 145.81	51023 ± 207.48	421553 ± 592.89

Table 6.13: Number of events per bin for the $|\cos\chi_{\text{BZ}}|$ distribution from the ALEPH data. The events at detector level (DL) from the full MC simulation and at hadron level (HL) are also given since these are the distributions used to calculate the detector corrections.

Fit Range

The sensitivity of the measurement to the fit range is checked by repeating the analysis with the requirement of a total correction per bin smaller than 20% (it was 10% in the standard analysis). The systematic variation due to this new fit range, see Table 6.18, is smaller than the statistical errors of the measurement showing that the range chosen for the nominal fit does not introduce any important bias in the measurement.

Selection Criteria

All cuts imposed in the selection of hadronic events have been moved in order to evaluate the effect on the measurement. The new values for the selection cuts on track parameters

Center of bin	N_{events} (ALEPH data)	N_{events} (full MC)	N_{events} (at HL)
-0.95	11846 ± 104.81	23557 ± 147.84	211284 ± 440.10
-0.85	7938 ± 86.90	15814 ± 122.67	128190 ± 348.88
-0.75	7527 ± 84.73	15303 ± 120.77	121960 ± 340.73
-0.65	7539 ± 84.80	15135 ± 120.14	119118 ± 336.94
-0.55	7540 ± 84.80	15190 ± 120.35	117738 ± 335.07
-0.45	7491 ± 84.54	15342 ± 120.92	116120 ± 332.88
-0.35	7768 ± 86.01	14966 ± 119.50	113898 ± 329.83
-0.25	7698 ± 85.64	14780 ± 118.79	111499 ± 326.50
-0.15	7868 ± 86.53	15049 ± 119.81	110124 ± 324.57
-0.05	8050 ± 87.48	15335 ± 120.89	112062 ± 327.28
0.05	7220 ± 83.07	13799 ± 114.96	100295 ± 310.37
0.15	6775 ± 80.58	12680 ± 110.40	96427 ± 304.57
0.25	6537 ± 79.21	12507 ± 109.67	95340 ± 302.92
0.35	6112 ± 76.70	12638 ± 110.22	95270 ± 302.81
0.45	6325 ± 77.97	12646 ± 110.26	96998 ± 305.43
0.55	6286 ± 77.74	12832 ± 111.03	100762 ± 311.06
0.65	6721 ± 80.27	13662 ± 114.41	106079 ± 318.82
0.75	7341 ± 83.73	15448 ± 121.31	118312 ± 335.85
0.85	8942 ± 91.93	18621 ± 132.51	144837 ± 369.55
0.95	19439 ± 130.84	41197 ± 189.73	320871 ± 529.43

Table 6.14: Number of events per bin for the $\cos\Phi_{\text{KSW}}$ distribution from the ALEPH data. The events at detector level (DL) from the full MC simulation and at hadron level (HL) are also given since these are the distributions used to calculate the detector corrections.

are found by changing them until the number of selected events per unit luminosity is the same in data and MC [54]. The analysis has been repeated by introducing the following changes (only one at a time): at least six measured space coordinates from the TPC; a polar angle at the origin in the range $20^\circ < \theta < 160^\circ$ both for charged and neutral tracks; transverse momentum $p_t > 0.205$ GeV/c; $d_0 = 1.867$cm; $z_0 = 6.64$cm; at least 8 selected charged tracks; minimum charged energy 22 GeV; $|\cos\Theta_{\text{Sph}}| < 0.85$; and fraction of electromagnetic energy $< 20\%$.

The observed changes when modifying the selection cuts are in general small and in many cases even negligible. The largest are at the 1% level for x and 2% for y (always below 1% for η).

Center of bin	N_{events} (ALEPH data)	N_{events} (full MC)	N_{events} (at HL)
0.025	6200 ± 77.23	11843 ± 106.83	89238 ± 293.43
0.075	6190 ± 77.18	11936 ± 107.24	89041 ± 293.12
0.125	6130 ± 76.81	12182 ± 108.29	89840 ± 294.38
0.175	6238 ± 77.45	12067 ± 107.80	91318 ± 296.70
0.225	6420 ± 78.53	12412 ± 109.27	93122 ± 299.51
0.275	6419 ± 78.52	12944 ± 111.49	95685 ± 303.44
0.325	6609 ± 79.63	13228 ± 112.66	99272 ± 308.85
0.375	6742 ± 80.39	13615 ± 114.22	102727 ± 313.96
0.425	7026 ± 81.99	14187 ± 116.49	107132 ± 320.33
0.475	7409 ± 84.10	14740 ± 118.64	112619 ± 328.06
0.525	7622 ± 85.24	15627 ± 121.98	118650 ± 336.31
0.575	7929 ± 86.85	15862 ± 122.85	126402 ± 346.56
0.625	8407 ± 89.29	16927 ± 126.69	133769 ± 355.97
0.675	8815 ± 91.31	17958 ± 130.27	143053 ± 367.41
0.725	9349 ± 93.88	18976 ± 133.69	152675 ± 378.80
0.775	9930 ± 96.57	20014 ± 137.07	161141 ± 388.47
0.825	10258 ± 98.04	20967 ± 140.07	168721 ± 396.87
0.875	10760 ± 100.25	21398 ± 141.41	170895 ± 399.23
0.925	10991 ± 101.24	22219 ± 143.90	177028 ± 405.81
0.975	13519 ± 111.34	27399 ± 158.43	215177 ± 443.77

Table 6.15: Number of events per bin for the $|\cos\theta_{\text{NR}}|$ distribution from the ALEPH data. The events at detector level (DL) from the full MC simulation and at hadron level (HL) are also given since these are the distributions used to calculate the detector corrections.

The total experimental systematic uncertainty is the quadratic sum of all contributions in Table 6.19, where individual contributions are calculated in the Bayesian approach. It results in 0.0002 for η, as well as 0.02 and 0.01 for the color factor ratios, x and y.

Hadronization and Background Corrections

The hadronization uncertainty is taken as the change in the fitted parameters when the corrections are calculated with HERWIG. The values can be found in Table 6.20 and show large systematic variations, up to 8.5% for y. The strong increase in the χ^2 when using

Center of bin	N_{events} (ALEPH data)	N_{events} (full MC)	N_{events} (at HL)
-0.95	11901 ± 105.03	26388 ± 155.74	194722 ± 424.00
-0.85	10876 ± 100.75	23119 ± 146.57	176953 ± 405.73
-0.75	10118 ± 97.42	21405 ± 141.43	166084 ± 393.97
-0.65	9460 ± 94.40	19943 ± 136.84	156041 ± 382.68
-0.55	9069 ± 92.54	18834 ± 133.22	146238 ± 371.23
-0.45	8778 ± 91.13	17892 ± 130.04	138956 ± 362.42
-0.35	8663 ± 90.57	16831 ± 126.35	132395 ± 354.24
-0.25	8472 ± 89.62	16366 ± 124.68	127638 ± 348.16
-0.15	8536 ± 89.94	16045 ± 123.52	123478 ± 342.74
-0.05	8553 ± 90.02	16032 ± 123.47	122407 ± 341.32
0.05	8654 ± 90.52	15858 ± 122.83	121501 ± 340.12
0.15	8573 ± 90.12	15873 ± 122.89	122513 ± 341.46
0.25	8701 ± 90.75	16337 ± 124.58	125502 ± 345.39
0.35	8706 ± 90.78	16404 ± 124.82	126296 ± 346.42
0.45	8601 ± 90.26	16535 ± 125.29	129140 ± 350.10
0.55	8376 ± 89.14	16359 ± 124.66	130377 ± 351.68
0.65	7634 ± 85.30	15844 ± 122.78	126767 ± 347.04
0.75	6194 ± 77.19	13351 ± 113.16	110759 ± 325.46
0.85	2961 ± 53.92	6727 ± 81.17	56819 ± 235.68
0.95	137 ± 11.70	358 ± 18.91	2920 ± 54.01

Table 6.16: Number of events per bin for the $\cos\alpha_{34}$ distribution from the ALEPH data. The events at detector level (DL) from the full MC simulation and at hadron level (HL) are also given since these are the distributions used to calculate the detector corrections.

$\eta(\mathrm{M_Z})$	x	y	χ^2/N_{dof}
0.0255 ± 0.0003	2.17 ± 0.06	0.37 ± 0.02	76.8/80

$\rho_{\eta y}$	ρ_{xy}
-0.450	0.845

Table 6.17: Results for the combined fit using ALEPH data.

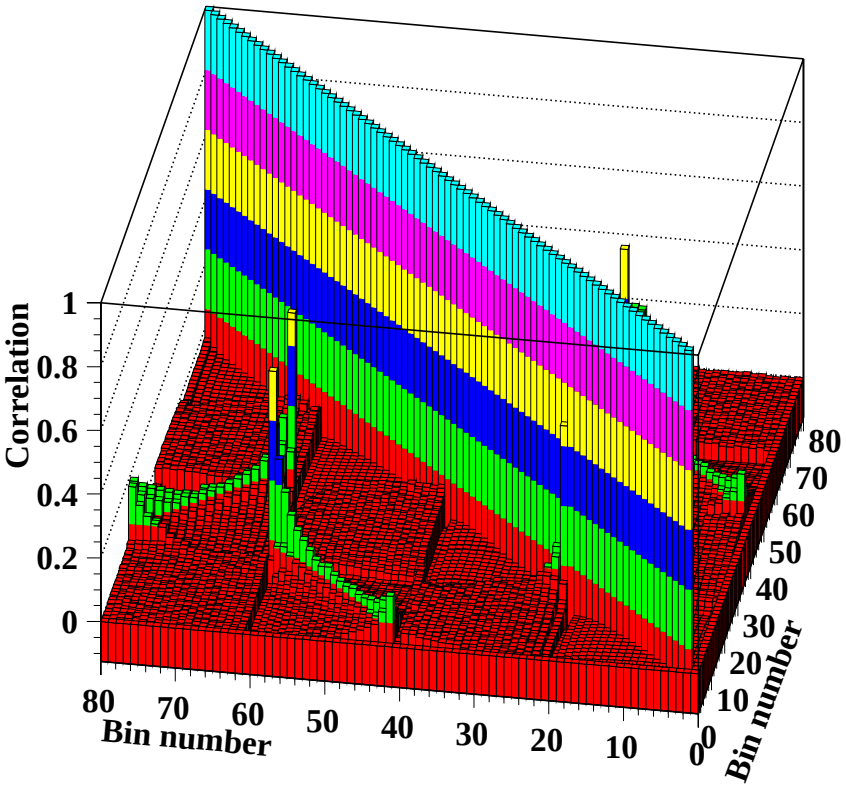

Figure 6.12: Bin-by-bin statistical correlations for the four-jet angular correlations. The numbers in the axis are the bin number: bins from 1 to 20 correspond to $|\cos\chi_{\mathrm{BZ}}|$, bins from 21 to 40 to $\cos\Phi_{\mathrm{KSW}}$, bins from 41 to 60 to $|\cos\theta_{\mathrm{NR}}|$ and bins from 61 to 80 to $\cos\alpha_{34}$.

	$\eta(\mathrm{M_Z})$	x	y	χ^2/N_{dof}
tot.corr. $< 20\%$	0.02565 ± 0.00021	2.191 ± 0.056	0.387 ± 0.019	89.0/88
Range sys.	$\Delta\eta = 0.0001$	$\Delta x = 0.02$	$\Delta y = 0.02$	

$\rho_{\eta y}$	ρ_{xy}
1.	1.

Table 6.18: Results when changing the fit range. The total corrections are chosen to be smaller than 20% instead of 10%.

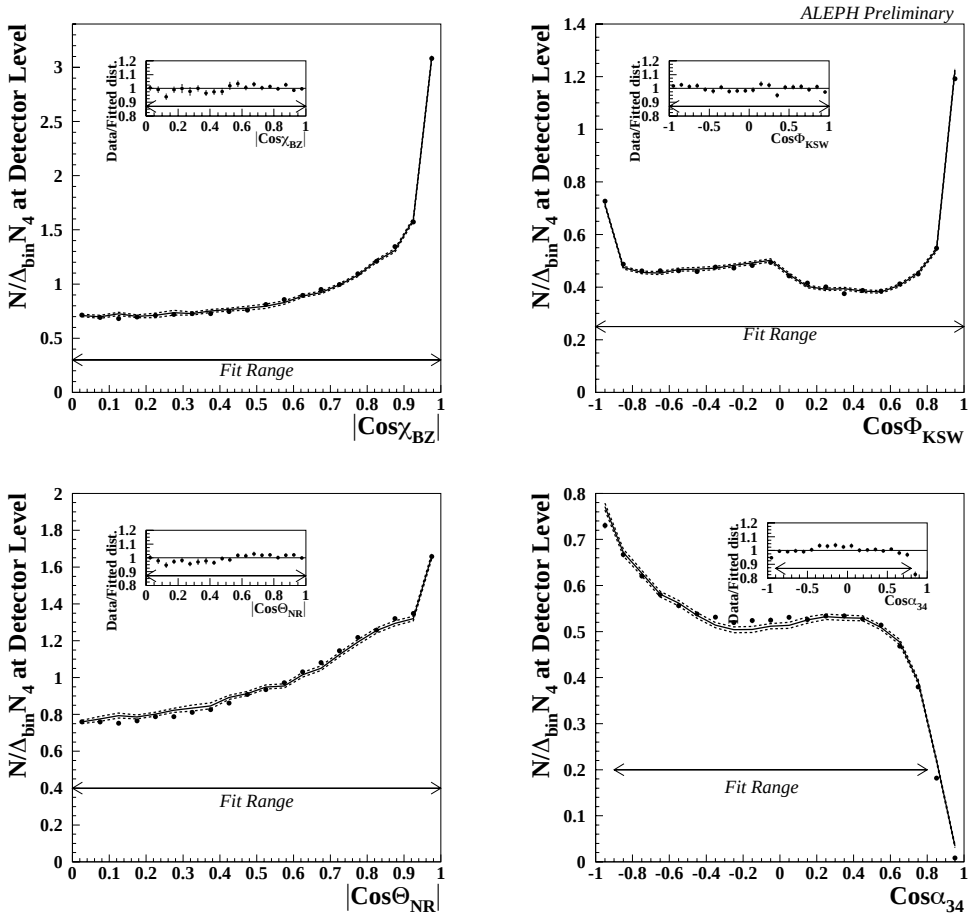

Figure 6.13: Comparison of ALEPH data and fit results for the angular correlations in four-jet events. The curves are obtained at detector level. Full dots correspond to ALEPH data. The solid lines show the fitted distributions while dashed lines correspond to their statistical uncertainty. The ratio of data with respect to fitted distributions is shown in the small inserts.

the corrections from HERWIG for the angular observables is an indication for unresolved issues in this new four-parton option.

Detector Corrections

An estimation of the systematic uncertainty due to the detector corrections has been obtained by repeating the analysis using charged tracks only. This change in the measurement procedure leads to systematic deviations on the parameters of about 1% for η and x, and about 3% for y.

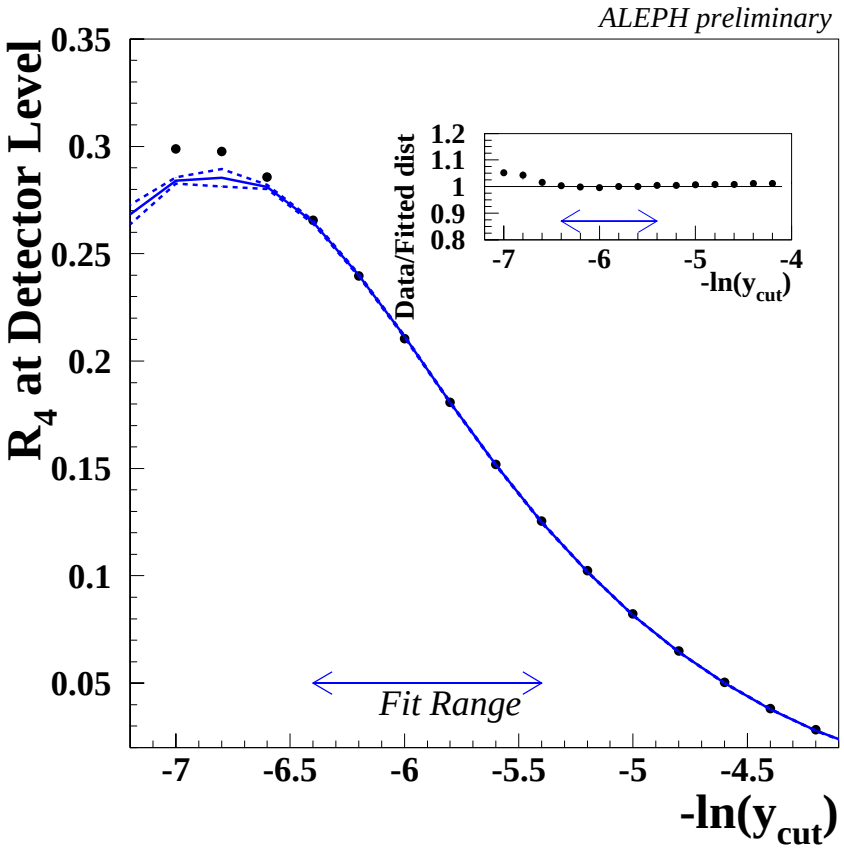

Figure 6.14: Comparison of ALEPH data and fit results for the four-jet rate. The curves are obtained at detector level. As in the previous figure, full dots correspond to ALEPH data and the solid line to the fitted distribution. The dashed lines are also plotted, however they are indistinguishable from the solid line for most of the y_{cut} range. Again, the ratio of data with respect to fitted distributions is shown in the small insert.

Another estimate is obtained by means of the four-parton full MC simulation described in Section 5.3.2. As explained, this new simulation is only used to correct $\cos\alpha_{34}$. It results in deviations similar to using charged tracks only.

The final uncertainty due to detector corrections, quoted in Table 6.21, is calculated by taking into account the two sources described above.

Theoretical Predictions

The lack of knowledge of higher order perturbative QCD is estimated by varying the renormalization scale in the theoretical predictions. The scale is varied from x_μ= 0.5

	$\eta(M_Z)$	x	y	χ^2/N_{dof}
Sphericity cut	0.02559 ± 0.00031	2.172 ± 0.064	0.373 ± 0.020	71.9/80
TPC cut	0.02540 ± 0.00030	2.166 ± 0.062	0.362 ± 0.020	76.3/80
N_{ch} cut	0.02562 ± 0.00031	2.151 ± 0.062	0.363 ± 0.020	84.6/80
E_{ch} cut	0.02551 ± 0.00031	2.179 ± 0.063	0.373 ± 0.020	75.9/80
θ_{ch} cut	0.02568 ± 0.00031	2.167 ± 0.062	0.376 ± 0.020	75.8/80
θ_{nt} cut	0.02556 ± 0.00031	2.155 ± 0.062	0.366 ± 0.020	81.1/80
Fraction of e.m. energy cut	0.02553 ± 0.00031	2.163 ± 0.062	0.366 ± 0.020	77.3/80
z_0 cut	0.02553 ± 0.00031	2.168 ± 0.062	0.369 ± 0.020	78.0/80
d_0 cut	0.02553 ± 0.00031	2.168 ± 0.062	0.369 ± 0.020	76.9/80
p_t cut	0.02549 ± 0.00031	2.169 ± 0.062	0.368 ± 0.020	79.1/80
Experimental sys.	$\Delta\eta = 0.0002$	$\Delta x = 0.02$	$\Delta y = 0.01$	

$\rho_{\eta y}$	ρ_{xy}
0.766	0.532

Table 6.19: Systematic uncertainties due to the selection cuts used in the analysis.

	$\eta(M_Z)$	x	y	χ^2/N_{dof}
HERWIG - all	0.02592 ± 0.00033	2.207 ± 0.072	0.428 ± 0.023	432./80
HERWIG - angles, PYTHIA - R_4	0.02508 ± 0.00032	2.225 ± 0.071	0.370 ± 0.023	412./80
PYTHIA - angles, HERWIG - R_4	0.02639 ± 0.00033	2.135 ± 0.064	0.417 ± 0.020	79.1/80
Background & Hadronization Sys.	$\Delta\eta = 0.0006$	$\Delta x = 0.02$	$\Delta y = 0.03$	

$\rho_{\eta y}$	ρ_{xy}
0.797	0.158

Table 6.20: Systematic uncertainties due to the background and hadronization corrections.

to x_μ=2, and the largest difference to the value found for x_μ=1 is taken as systematic uncertainty. As the theoretical predictions for R_4 and for the angular correlations are known at different accuracy, the scale uncertainty is estimated by varying x_μ separately for each of the two kind of observables. The resulting uncertainty is 4% for η, 2% for x and 13% for y. It is the dominant one for the first and third parameters.

	$\eta(M_Z)$	x	y	χ^2/N_{dof}
Charged Only	0.02577 ± 0.00031	2.143 ± 0.062	0.359 ± 0.020	82.5/80
4-partons Full MC	0.02583 ± 0.00031	2.089 ± 0.061	0.346 ± 0.020	101.1/80
Detector sys.	$\Delta\eta = 0.0001$	$\Delta x = 0.02$	$\Delta y = 0.01$	

$\rho_{\eta y}$	ρ_{xy}
-0.896	0.991

Table 6.21: Systematic uncertainties due to detector effects.

The experimentally optimized scale method, which was used for the measurement of the strong coupling from the four-jet rate, is not used for the combined measurement for several reasons. First, the normalized angular correlations have been used due to the lack of the resummation of large logarithms. The normalized observables are expected to have a small scale dependence, as this is cancelled out in the normalization by the NLO four-jet cross section. Then, at least two different scales should be fitted, one for the four-jet rate and another for the angular observables. Second, since the colour factors and x_μ are highly correlated, the addition of this new variable introduces instabilities in the fit. Finally, even if the predictions for all four-jet angular correlations are known at NLO, the optimized scale for each observable can take on different values.

An evaluation of mass effects, which are not included in the theoretical predictions, is attempted by using the FOURJPHACT MC program [58]. As the parameters for PYTHIA were optimized for massless partons, the hadronization and background corrections with massive partons for the angular observables are calculated as follows,

$$C^{\mathrm{bck+had}}(i_{bin}) = \frac{\cos X^{\mathrm{part-4j}}(i_{bin})}{\cos X^{\mathrm{part-py}}(i_{bin})} \frac{\cos X^{\mathrm{had-py}}(i_{bin})}{\cos X^{\mathrm{part-py}}(i_{bin})} \quad , \tag{6.3}$$

where the index part-4j indicates the parton level coming from FOURJPHACT, and part-py (had-py) the parton (hadron) level from PYTHIA. The first ratio corrects for mass effects in the LO prediction, and the second ratio assumes that the showering and hadronization corrections do not depend strongly on the quark masses. It is found that mass effects might be large, up to 0.07 for x.

The total theoretical uncertainty, see Table 6.22, is obtained adding quadratically the contribution of the two sources described above and results in the dominant systematic uncertainty for all parameters.

	$\eta(M_Z)$	x	y	χ^2/N_{dof}
x_μ=0.5 for the angles	0.02545 ± 0.00032	2.193 ± 0.067	0.377 ± 0.021	64.8/80
x_μ=2. for the angles	0.02558 ± 0.00030	2.148 ± 0.059	0.361 ± 0.019	87.9/80
x_μ=0.5 for R_4	0.02352 ± 0.00030	2.265 ± 0.062	0.266 ± 0.018	72.6/80
x_μ=2. for R_4	0.02712 ± 0.00031	2.096 ± 0.063	0.439 ± 0.021	86.8/80
scale sys.	$\Delta\eta = 0.0010$	$\Delta x = 0.051$	$\Delta y = 0.05$	
quark masses	0.02629 ± 0.00035	1.982 ± 0.062	0.317 ± 0.020	84.1/80
mass sys.	$\Delta\eta = 0.0003$	$\Delta x = 0.07$	$\Delta y = 0.02$	
Theoretical sys.	$\Delta\eta = 0.0010$	$\Delta x = 0.09$	$\Delta y = 0.05$	

$\rho_{\eta y}$	ρ_{xy}
0.792	-0.212

Table 6.22: Systematic uncertainties due to variations in the theoretical predictions.

6.2.4 Further Checks

Hadronization and Background Corrections

As a cross-check, the more extreme models presented in Sect. 5.3.1 were used to fit η and the color factor ratios. The systematic changes in the fitted parameters, see Table 6.23, would be of about 2-3%, which is covered by the total uncertainty. Finally, also the standard PYTHIA simulation, $q\bar{q}$ + PS + hadronization, has been used to correct the four-jet angular correlations (again Table 6.23). As expected, the χ^2 of the fit is much larger than the one of the standard fit showing that the PYTHIA simulation which uses four-parton matrix elements and a parton shower describes better the shape of the angular correlations.

Two- and Three-Parton Backgrounds for the Angular Correlations

The background and hadronization corrections used for the angular correlations are valid provided that the number of two- and three-parton events that are clustered into four jets after hadronization is negligible. This is verified by the following study.

Using the PYTHIA ME option as described in Section 5.3.1, 1 million events were generated. The hadronization parameters were the standard ones. The fraction of the

	$\eta(M_Z)$	x	y	χ^2/N_{dof}
ME - all	0.02787 ± 0.00036	1.967 ± 0.066	0.343 ± 0.020	96.1/80
ME - angles, PYTHIA - R_4	0.02632 ± 0.00034	1.979 ± 0.065	0.317 ± 0.020	98.3/80
PYTHIA - angles, ME - R_4	0.02702 ± 0.00032	2.154 ± 0.063	0.394 ± 0.020	76.9/80
PYTHIA,Q_0 - R_4	0.02749 ± 0.00034	2.111 ± 0.063	0.423 ± 0.020	90.0/80
PYTHIA $q\bar{q}$ - all	0.02639 ± 0.00033	1.92 ± 0.064	0.293 ± 0.020	162.1/80

Table 6.23: Check for the Hadronization and Background corrections. Deviations from the standard analysis are covered by the systematic uncertainties already described.

number of four-jet events at HL which came from two- and three-parton events with respect to the total number of four-jet events was found to be much smaller than 1%, and only slightly affecting the shape of the angular correlations as observed in Fig. 6.15.

In order to quantify how the two- and three-parton backgrounds could bias our measurement the four-jet angular correlations obtained at HL, from the PYTHIA ME simulation, were fitted. The hadronization corrections were calculated using the PYTHIA four-parton simulation. Then, from those distributions the background contributions were subtracted (dashed distributions in Fig. 6.15), and the resulting ones are fitted again. The difference between the fitted parameters can be taken as an estimate of the two- and three-parton background uncertainty. As seen in the Table 6.24, the systematic uncertainties for the different parameters are much smaller than the ones considered in the previous section. Therefore, no further two- and three-parton background treatment was implemented in the analysis.

	$\eta(M_Z)$	x	y	χ^2/N_{dof}
Full HL distrib.	0.02580 ± 0.00027	2.022 ± 0.048	0.308 ± 0.016	115.1/81
Without 2- & 3-parton bckg	0.02582 ± 0.00028	2.018 ± 0.048	0.308 ± 0.016	111.2/81

Table 6.24: Check for two- and three-parton background effects.

Sensitivity Checks

The sensitivity of the analysis to each of the observables is studied. The fit results when taking out one observable at a time can be seen in Table 6.25. As expected, η is mainly fixed by the R_4 distribution, and the color factor ratios by the angular correlations. The

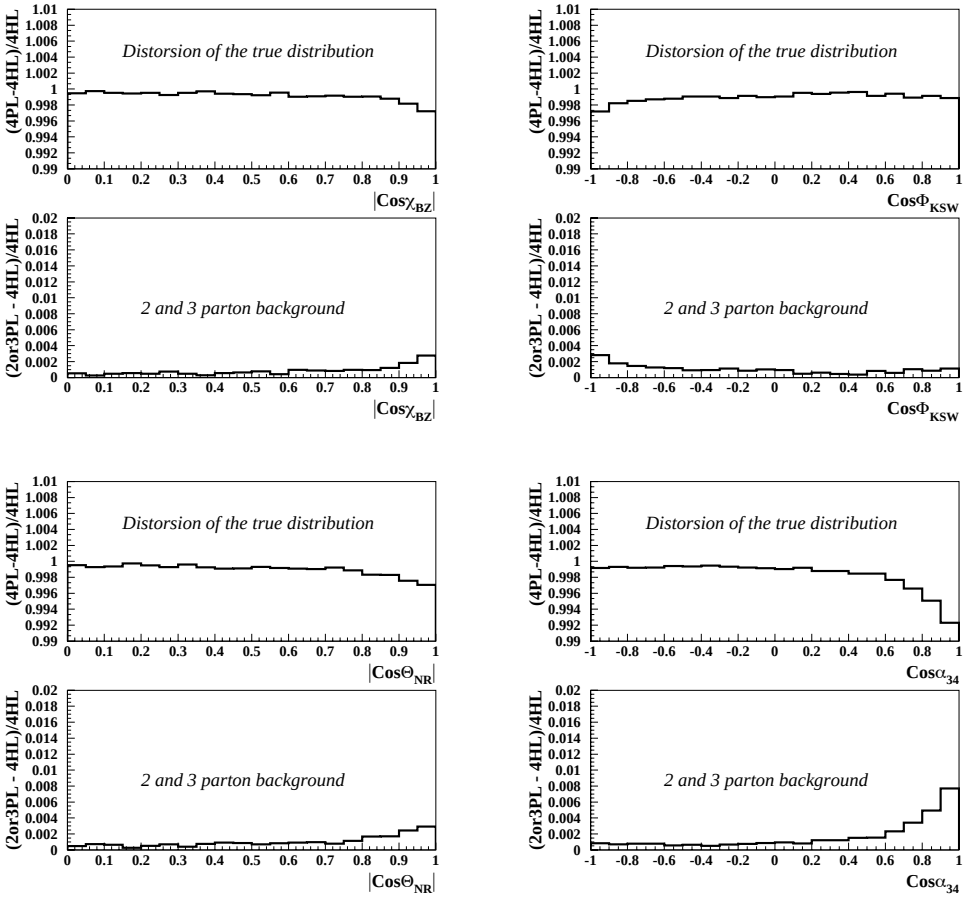

Figure 6.15: Distortion in the four-jet angular correlations due to two- and three-parton backgrounds.

sensitivity to the different angular correlations is quite similar. The fit with the angular correlations only resulted in a nonsense *eta*, for which the error could not be calculated.

	$\eta(\mathrm{M_Z})$	x	y	χ^2/N_{dof}
No $\cos\chi_{\mathrm{BZ}}$	0.0253 ± 0.0003	2.21 ± 0.08	0.38 ± 0.02	58.5/63
No $\cos\Phi_{\mathrm{KSW}}$	0.0256 ± 0.0003	2.12 ± 0.07	0.35 ± 0.02	52.6/60
No $\cos\Theta_{\mathrm{NR}}$	0.0255 ± 0.0003	2.19 ± 0.06	0.38 ± 0.02	59.1/60
No $\cos\alpha_{34}$	0.0255 ± 0.0003	2.16 ± 0.06	0.37 ± 0.02	66.1/60
No R_4	$0.0900 \pm - - -$	2.27 ± 0.09	0.37 ± 0.05	44.2/74

Table 6.25: Results from the sensitivity check. The analysis is repeated taking out one of the observables at a time.

Dependence on the y_{cut}

A check was performed in order to see if the present measurement depends on the chosen value of y_{cut}. The analysis is repeated with the four-jet events calculated for $y_{cut} = 0.01$, which represents a drop in the four-jet rate from 7.1% for the standard 0.008 y_{cut} value to 5.4%. The results are given in Table 6.26 and are in good agreement with the standard analysis.

	$\eta(M_Z)$	x	y	χ^2/N_{dof}
y_{cut}=0.01	0.0259 ± 0.0004	2.15 ± 0.08	0.34 ± 0.02	99.5/81

Table 6.26: Results for the fit when y_{cut} is fixed to 0.01 instead of 0.008 as used for the standard analysis.

6.2.5 Final Results

Putting together all systematic uncertainties considered above, the final result of the combined measurement of η and the colour factors ratios is:

$$\begin{aligned} \eta(M_Z) &= 0.0255 \pm 0.0003(stat) \pm 0.0012(sys) \\ x &= 2.17 \pm 0.06(stat) \pm 0.10(sys) \\ y &= 0.37 \pm 0.02(stat) \pm 0.06(sys) \end{aligned}$$

$$\begin{aligned} (\rho_{\eta y})_{stat} &= -0.450 \qquad (\rho_{\eta y})_{sys} = 0.769 \\ (\rho_{xy})_{stat} &= 0.845 \qquad (\rho_{xy})_{sys} = -0.028 \end{aligned}$$

which can also be expressed in terms of the strong coupling constant and the colour factors,

$$\begin{aligned} \alpha_s(M_Z) &= 0.119 \pm 0.006(stat) \pm 0.022(sys) \\ C_A &= 2.93 \pm 0.14(stat) \pm 0.50(sys) \\ C_F &= 1.35 \pm 0.07(stat) \pm 0.22(sys) \end{aligned}$$

These results are in good agreement with previous measurements. The dominant source of systematic uncertainty is obtained from variations in the theoretical predictions, where both the scale and the quark mass effects result in large deviations from the standard measurement.

Figure 6.16 shows that the measurement of the colour factor ratios is in agreement with the expectations from QCD (x=2.25 and y=0.375). The agreement with previous measurements by ALEPH [21] and lately by OPAL [55] is also observed. The total systematic errors are similar to the ones of previous analyses, but the statistical uncertainty has been strongly reduced because of the specific method adopted here.

Finally, Fig. 6.17 shows the fitted colour factor ratios for the systematic uncertainties considered in the analysis as well as for most of the further checks listed in Section 6.2.4. The compatibility of all variations with the standard fit is observed.

6.3 Massless Gluino Hypothesis

A final study was carried out in order to test the hypothesis of the existence of a massless gluino. As in the measurement described above, DEBRECEN is used to obtain the NLO perturbative prediction. This MC program provides not only the B and C functions for pure QCD, but also for QCD+massless gluino. Only the four-jet angular correlations have been used, since there is no consistent prediction for R_4, for which gluino contributions are not available in the resummation terms.

The simultaneous measurement of the strong coupling constant and the colour factors has been repeated using as perturbative predictions for the four-jet angular correlations the ones outlined in Eq. 3.22. Two cases have been considered. First, the B and C functions were taking into account only pure QCD configurations. Then the gluino contributions were also included in these functions, and the QCD beta function coefficients in Eq. 2.14 where changed to [20],

$$\begin{aligned} \beta_0 &= \frac{11}{3}x - \frac{4}{3}\left(yN_f + x\frac{N_g}{2}\right), \\ \beta_1 &= \frac{17}{3}x^2 - 2\left(y\,N_f + x^2\frac{N_g}{2}\right) - \frac{10}{3}\left(x\,y\,N_f + x^2\frac{N_g}{2}\right). \end{aligned} \tag{6.4}$$

where N_g is the number of gluinos, set to 1 in this analysis.

Hadronization and detector corrections were taken from the standard analysis under the assumption that they are not strongly dependent on the gluino contribution. At the moment of writing this work, there is no MC program which models the gluino contributions to hadronization. All the studies of systematic uncertainties described in

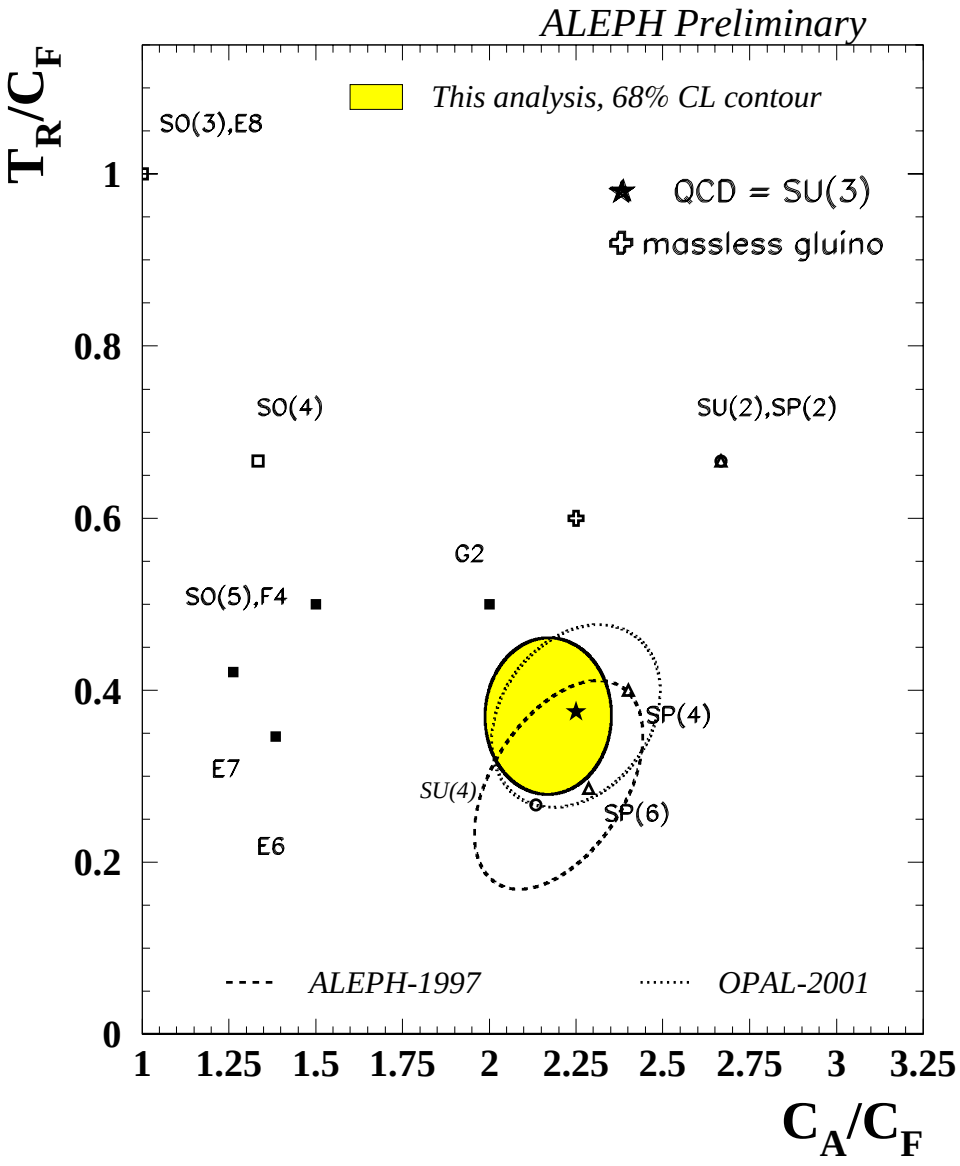

Figure 6.16: 68% confidence level contour in the (x,y) plane, calculated from statistical plus systematic errors (shaded region). For comparison also the results from previous measurements are given, as well as predictions for simple Lie groups.

Section 6.2.3 have been repeated.

The results of the fit together with an estimate of the systematic uncertainties are

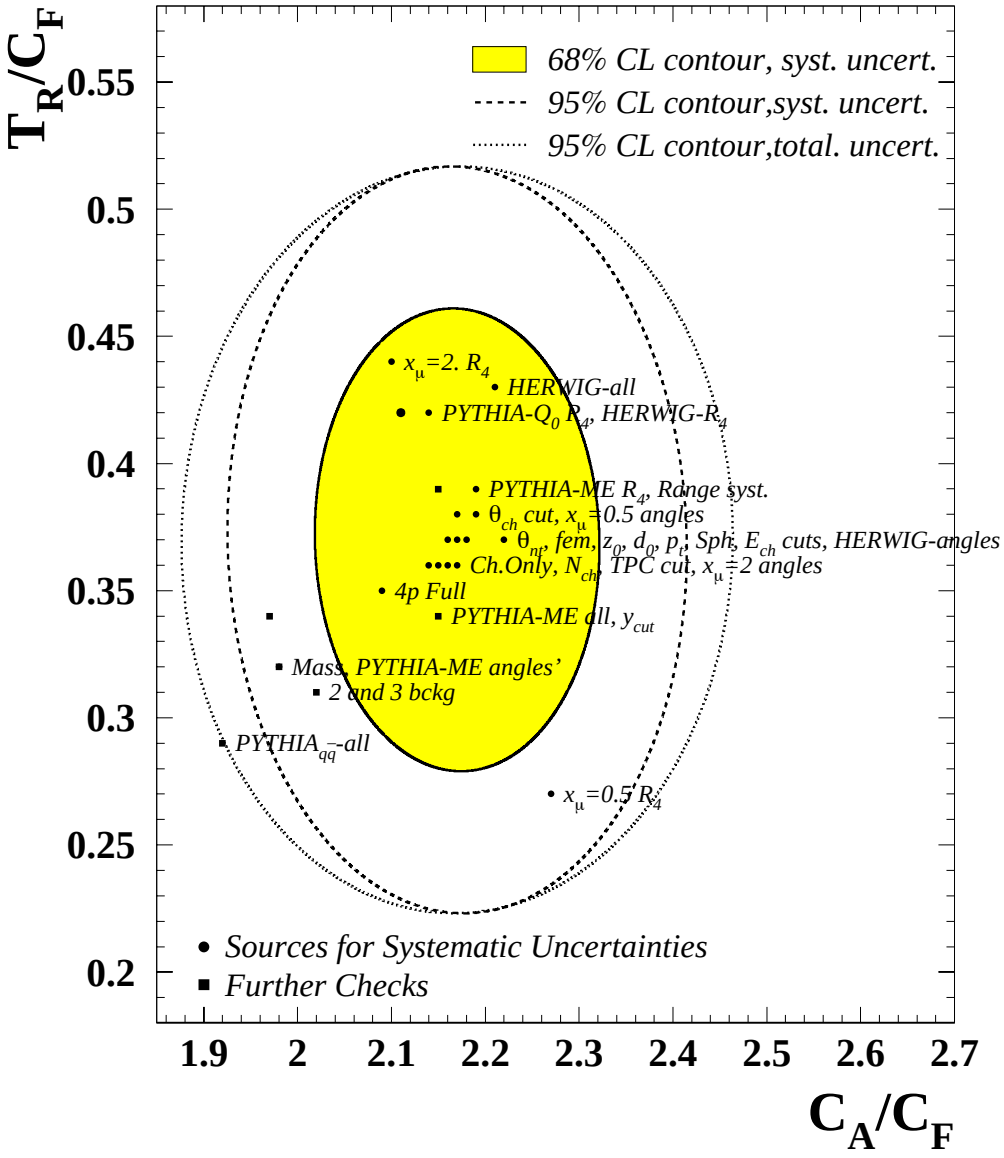

Figure 6.17: 68% and 95% confidence level contours in the (x,y) plane when taking into account systematic uncertainties only. The 95% confidence level contour with the total uncertainty is shown for comparison. Results for the sources of systematic uncertainty are also plotted.

$$x = 2.27 \pm 0.09(\text{stat}) \pm 0.08(\text{sys})$$
$$y = 0.38 \pm 0.05(\text{stat}) \pm 0.07(\text{sys})$$
$$(\rho_{xy})_{\text{total}} = -0.145$$

for the pure QCD case, and

$$x = 2.26 \pm 0.08(\text{stat}) \pm 0.07(\text{sys})$$
$$y = 0.15 \pm 0.06(\text{stat}) \pm 0.06(\text{sys})$$
$$(\rho_{xy})_{\text{total}} = -0.187$$

for the QCD+gluino hypothesis. The reduction of the total systematic uncertainty for x with respect to the standard fit comes from the lack of one of the contributions to the theoretical uncertainty estimate, namely the scale uncertainty for the four-jet rate.

Figure 6.18 shows that these results exclude the existence of a massless gluino at more than 95% confidence level, since the measured colour factor ratios do not agree with $SU(3)$ anymore. It is worth noting that effects of a massive gluino have not been studied in this thesis, since no NLO predictions including mass terms are available.

6.4 Conclusions

Results were presented for a measurement of the strong coupling constant from the four-jet rate as obtained by the Durham clustering algorithm (E-scheme). The result for $\alpha_{\text{s}}(\text{M}_{\text{Z}})$ using 1994-95 ALEPH data is:

$$\alpha_{\text{s}}(\text{M}_{\text{Z}}) = 0.1170 \pm 0.0001(stat) \pm 0.0014(sys) \quad ,$$

with the renormalization scale $x_\mu = 1$.

However, data shows a preference for x_μ values smaller than 1, as can be seen when α_{s} and x_μ are fitted simultaneously. In this case the results are

$$\alpha_{\text{s}}(\text{M}_{\text{Z}}) = 0.1175 \pm 0.0002(stat) \pm 0.0006(sys)$$
$$x_\mu = 0.73 \pm 0.05,$$

where the error on x_μ is statistical only. The preferred small x_μ indicates that missing higher order corrections are still important.

These results are in perfect agreement with previous measurements based on three-jet quantities [9][54].

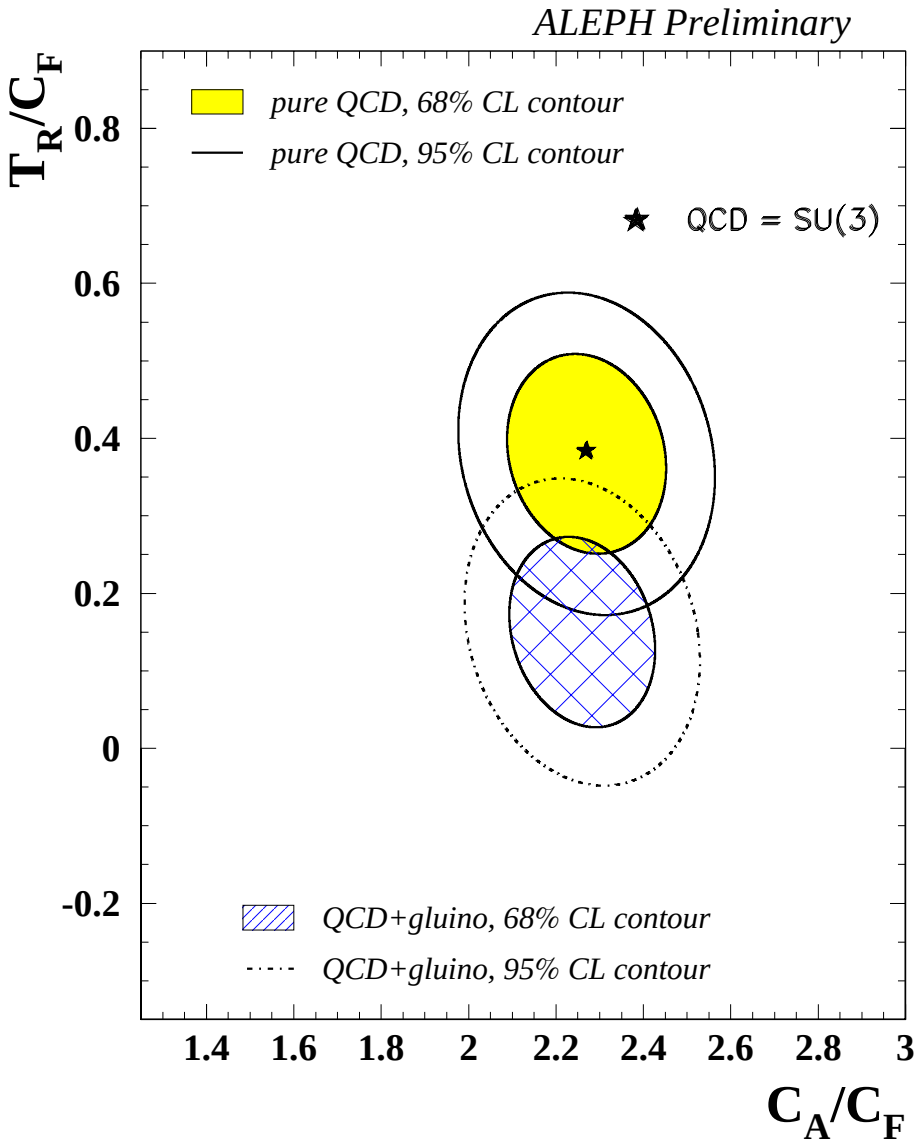

Figure 6.18: 68% and 95% confidence level contours in the (x,y) plane for the QCD and QCD+gluino hypotheses, based on four-jet angular correlations. The uncertainties include statistical as well as systematic errors.

A combined measurement of the strong coupling constant and the colour factors from angular correlations in four-jet events and the four-jet rate has been presented. For the jet finding the Durham clustering algorithm (E-scheme) was used, with y_{cut}=0.008 for the four-jet events used to compute the angular correlations. The results are

$$\alpha_s(M_Z) = 0.119 \pm 0.006(stat) \pm 0.022(sys)$$
$$C_A = 2.93 \pm 0.14(stat) \pm 0.50(sys)$$

$$C_F = 1.35 \pm 0.07(stat) \pm 0.22(sys)$$

These results are in good agreement with previous measurements, with similar systematic uncertainties, but with an important reduction in the statistical error.

Large discrepancies have been found when using either PYTHIA or HERWIG predictions for the calculations of hadronization corrections to the angular correlations. This indicates some problem either in the tuning or in the showering and hadronization implementation in these MC programs. The problems in the description of the shape for $\cos\alpha_{34}$ are further hints together with the worsening of the shape of the $|\cos\Theta_{\mathrm{NR}}|$ shape when using a full simulation starting from four-parton massless MEs.